# Amorphous thin film growth: Minimal deposition equation

Martin Raible, Stefan J. Linz, and Peter Hänggi
*Theoretische Physik I, Institut für Physik, Universität Augsburg, D-86135 Augsburg, Germany*
(Received 3 March 2000)

A nonlinear stochastic growth equation is derived from (i) the symmetry principles relevant for the growth of vapor deposited amorphous films, (ii) no excess velocity, and (iii) a low-order expansion in the gradients of the surface profile. A growth instability in the equation is attributed to the deflection of the initially perpendicular incident particles due to attractive forces between the surface atoms and the incident particles. The stationary solutions of the deterministic limit of the equation and their stability are analyzed. The growth of the surface roughness and the correlation length of the moundlike surface structure arising from the stochastic growth equation is investigated.

PACS number(s): 68.35.Bs, 61.43.Dq

## I. INTRODUCTION

The understanding of the kinetics of surface growth processes has recently developed into a highly active research area of statistical physics (see Ref. [1]). The dynamics of the surface evolution, e.g., in molecular beam epitaxy (MBE) or physical vapor deposition is dominated by the competition between roughening mechanisms due to deposition of particles and smoothening mechanisms due to surface diffusion [2–6]. The growing surface can evolve into self-similar structures or, in the presence of a growth instability, into periodic patterns. In particular, the growth of amorphous thin films represents an attractive system for the understanding of surface growth processes because of the spatially isotropic nature of the amorphous structure and the absence of long range structural order. Experimental studies of amorphous thin films, deposited by electron beam evaporation, display the formation of moundlike structures on a mesoscopic length scale [7,8]. Despite the complexity of the growth process on the atomic scale this indicates that coarse-grained continuum models based on stochastic growth equations [1] can be useful for the understanding of the growth dynamics.

Our investigation focuses on the development and the analysis of a minimal deposition equation appropiate for the modeling of amorphous film growth under physical vapor deposition conditions (low-energetic particles) and normal incidence.

Our paper is organized as follows. In Sec. II we present the basic experimental setup under consideration and a summary of constructive elements leading to a heuristic ansatz for the deposition equation for amorphous film growth. In Sec. III, we use a systematic approach to obtain the minimal functional form of the deposition equation and relate the entering terms to their underlying surface relaxation mechanisms. This yields an additional justification of the heuristic ansatz in Sec. II. In Sec. IV, we give a thorough discussion of the existence and stability of the stationary solutions of the deterministic deposition equation which constitutes the skeleton of time evolution of the stochastic deposition equation. A detailed numerical investigation of the time evolution of the correlation length and the surface roughness resulting from the deposition equation is presented in Sec. V. Section VI summarizes the major results of our study.

## II. BASICS

As a tool for the theoretical description of the time evolution of the surface morphology $H(\vec{x},t)$ where $H$ denotes the $z$ coordinate of the growing surface at the substrate position $\vec{x}=(x,y)$ and time $t$ (see also Fig. 1), we use the well-established phenomenological approach that is based on stochastic nonlinear partial differential equations [1]

$$\partial_t H = G(\vec{\nabla} H) + F + \eta. \tag{1}$$

In Eq. (1), $G$ denotes a functional that contains the various surface relaxation phenomena and only depends on the derivatives of the surface height since the growth process is determined by the *local* surface properties. The functional form of $G$ depends strongly on the considered experimental setup and the details of the kinetics of the deposition process. Moreover, $F$ in Eq. (1) denotes the mean deposition rate and $\eta(\vec{x},t)$ is the corresponding deposition noise that determines the fluctuations of the deposition flux about its mean $F$. These fluctuations are assumed to be Gaussian white,

$$\langle \eta(\vec{x},t)\rangle = 0; \quad \langle \eta(\vec{x},t)\,\eta(\vec{y},t')\rangle = 2D\,\delta^d(\vec{x}-\vec{y})\,\delta(t-t'), \tag{2}$$

where the brackets denote ensemble averaging, $D$ the fluctuation strength, $d$ the spatial dimension of the surface ($d$

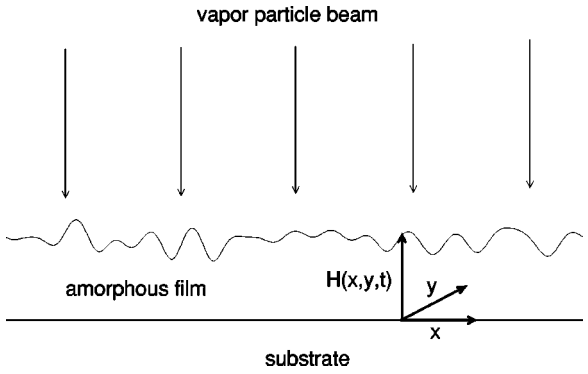


FIG. 1. Sketch of the vapor deposition of an amorphous film on a substrate.

 

$=1$ or 2). For an estimate of the magnitude of $D$ we refer to Appendix A. Moreover, it proves useful to introduce the height profile

$$h(\vec{x},t)=H(\vec{x},t)-Ft \tag{3}$$

in the frame comoving with the mean deposition rate $F$. Then, the spatiotemporal evolution of $h(\vec{x},t)$ is given by $\partial_t h=G(\vec{\nabla}h)+\eta$. If the deposition process has no excess velocity, $\langle\partial_t h\rangle=0$, there is a simple, linear relation between the mean growth or layer thickness $\langle H\rangle$ and time, $\langle H\rangle=Ft$, yielding $\langle h\rangle=0$. This assumption is justified if the substrate temperature is low enough to suppress particle desorption and if the film grows with constant density.

The simplest equation of this type, $\partial_t h=\nu\nabla^2 h+\eta$, was suggested by Edwards and Wilkinson [9] in order to describe the sedimentation of a granular aggregate in the presence of a gravitational field. In the context of surface growth phenomena, the desorption of particles from the surface could also cause the Laplacian term with positive $\nu$ [10]. This effect, however, is negligibly small at usual substrate temperatures used in vapor deposition experiments. Moreover, the experimentally observed moundlike surface structure [7,8] suggests the presence of a growth instability, i.e., $\nu<0$ as we shall argue in this paper. This kind of growth instability was proposed by Villain [3] as the consequence of a diffusion bias on the terraces of a crystalline layer due to a potential barrier at the step edges. Although this effect is absent in amorphous film growth, a term $\nu\nabla^2 h$ with negative $\nu$ can still appear due to the deflection of the initially perpendicular incident particles caused by the interatomic forces between the surface atoms and the incident particles, see Sec. III B.

Because the deposited particles prefer to relax at surface sites that offer the strongest binding, a surface current of the type $\vec{j}=K\vec{\nabla}(\nabla^2 h)$ adds the term $-K\nabla^4 h$ to the growth equation [2,4,10]. The resulting growth equation $\partial_t h=\nu\nabla^2 h-K\nabla^4 h+\eta$ with negative $\nu$ and positive $K$ needs to be supplemented by a nonlinear term to avoid exponential growth at large length scales. If the growth instability $\nu\nabla^2 h$ and the conserved Kardar-Parisi-Zhang (KPZ) equation $\partial_t h=-K\nabla^4 h+\lambda_1\nabla^2(\vec{\nabla}h)^2+\eta$ [3,5] are combined one obtains the stochastic field equation $\partial_t h=\nu\nabla^2 h-K\nabla^4 h+\lambda_1\nabla^2(\vec{\nabla}h)^2+\eta$, that has been proposed by Siegert and Plischke [6] as a continuum model for the MBE growth of crystalline layers in the presence of a step edge barrier. The nonlinear term $\lambda_1\nabla^2(\vec{\nabla}h)^2$ can be motivated by a surface current, that equilibrates the slope dependent adatom concentration [3].

For amorphous film growth, the adatom concentration depends on the surface slope because of a simple geometrical argument by Moske [11] (see Appendix B for a variant of this argument). If only freshly deposited particles are allowed to diffuse before their relaxation their surface concentration follows a behavior given by $n\sim 1/\sqrt{1+(\vec{\nabla}h)^2}\approx 1-(\vec{\nabla}h)^2/2$. This causes a diffusion current of the type $\vec{j}\sim-\vec{\nabla}n\sim\vec{\nabla}(\vec{\nabla}h)^2$ and leads to the $\lambda_1\nabla^2(\vec{\nabla}h)^2$ term with $\lambda_1<0$. This argument is also valid, if *additionally* thermally activated surface diffusion is present.

Therefore, after renaming of the coefficients, a reasonable heuristic model for the stochastic growth equation governing deposited amorphous thin films is determined by

$$\partial_t h=a_1\nabla^2 h+a_2\nabla^4 h+a_3\nabla^2(\vec{\nabla}h)^2+\eta \tag{4}$$

with negative coefficients $a_1$, $a_2$, and $a_3$.

## III. MODEL EQUATION

In this section, we first derive the simplest nonlinear functional form of the deterministic part of the surface growth equation using the symmetry principles governing the amorphous growth process, no excess velocity and a low-order expansion in the gradients of the height profile $h(\vec{x},t)$ (for the growth equation that allows for a finite excess velocity see Appendix D). Then we relate the various terms entering in this minimal deposition equation to microscopic processes governing the amorphous surface growth.

### A. Derivation of the minimal deposition equation

Following Ref. [1], the invariances under translation in time, translation along and perpendicular to the growth direction imply a phenomenological ansatz for the surface growth dynamics of the form $\partial_t h=G(\vec{\nabla}h)+\eta$. Here, the functional $G(\vec{\nabla}h)$ only depends on the gradients of $h(\vec{x})$, higher order spatial derivatives and their combinations. Moreover, the rotation and reflection invariance in the plane perpendicular to the growth direction, see Fig. 1, that reflects the isotropy of the amorphous phase determines $G(\vec{\nabla}h)$ to be a scalar, i.e., odd derivatives are ruled out and the $\vec{\nabla}$ operators must be multiplied in couples by scalar multiplication. If $G(\vec{\nabla}h)$ is not allowed to produce any excess velocity, it must be given by the divergence of a vector field, i.e., $G(\vec{\nabla}h)=-\vec{\nabla}\cdot\vec{j}(\vec{\nabla}h)$.

Next, we expand $G(\vec{\nabla}h)$ in orders of $h$ and $\vec{\nabla}$, following the aforementioned symmetry principles. The allowed linear terms are $\nabla^2 h$, $\nabla^4 h$, $\nabla^6 h$, etc. Only the first two of them are regarded in the following and terms of order $\mathcal{O}(\nabla^6)$ are omitted. Therefore, the first and the second term of $G(\vec{\nabla}h)$ read $a_1\nabla^2 h$ and $a_2\nabla^4 h$.

The only functional form of $G(\vec{\nabla}h)$ being quadratic in $h$ *and* $\vec{\nabla}$, not being explicitly dependent on $h$, and being a scalar reads $(\vec{\nabla}h)^2$. But this term (a KPZ nonlinearity [12]) does not satisfy the condition of no excess velocity. Therefore, the possible terms being quadratic in $h$ are at least of order $\mathcal{O}(\nabla^4)$. One obtains $\vec{\nabla}[(\vec{\nabla}\vec{\nabla}h)(\vec{\nabla}h)]$ as the common type of terms of order $\mathcal{O}(\nabla^4,h^2)$. Now, the $\nabla$-operators have to be multiplied in couples, yielding two combinations: $2b_3\vec{\nabla}\cdot[(\vec{\nabla}\vec{\nabla}h)\cdot(\vec{\nabla}h)]=b_3\nabla^2(\vec{\nabla}h)^2$ and $b_4\vec{\nabla}\cdot[(\vec{\nabla}h)(\nabla^2 h)]$. Other possible terms of $G(\vec{\nabla}h)$ are of order $\mathcal{O}(\nabla^6,h^3)$; we only mention that adding the term $\vec{\nabla}\cdot[(\vec{\nabla}h)(\vec{\nabla}h)^2]$ would complete the list of terms up to fourth order in $\vec{\nabla}$.

In summary, the functional form of $G(\vec{\nabla}h)$ is determined by

$$G(\vec{\nabla}h)=a_1\nabla^2h+a_2\nabla^4h+b_3\nabla^2(\vec{\nabla}h)^2+b_4\vec{\nabla}\cdot[(\vec{\nabla}h)(\nabla^2h)]+\mathcal{O}(\nabla^6,h^3). \quad (5)$$

Since the fourth term in Eq. (5) can be decomposed in the form

$$\vec{\nabla}\cdot[(\vec{\nabla}h)(\nabla^2h)]=\frac{1}{2}\nabla^2(\vec{\nabla}h)^2+2M \quad (6)$$

with

$$M=\det\begin{pmatrix}\partial_x^2h & \partial_y\partial_xh\\ \partial_x\partial_yh & \partial_y^2h\end{pmatrix} \quad (7)$$

the functional form of the lowest-order nonlinear deterministic surface growth equation reads after renaming of the coefficients

$$\partial_th=G(\vec{\nabla}h)=a_1\nabla^2h+a_2\nabla^4h+a_3\nabla^2(\vec{\nabla}h)^2+a_4M. \quad (8)$$

Apart from the term $a_4M$, the systematically derived deposition equation (8) coincides with the Heuristic ansatz (4). The last term in Eq. (8), $a_4M$, is only present in the two-dimensional case. In the one-dimensional case where $h$ only depends on one spatial coordinate, $M=0$ holds. As we shall see in the next section, the physical origin of the term $a_4M$ suggests that it is small and negligible. The two nonlinear terms $a_3\nabla^2(\vec{\nabla}h)^2$ and $a_4M$ in Eq. (8) both break the up/down symmetry of the height profile $h(\vec{x},t)$. Equation (8), however, is invariant with respect to the combined transformation $\{h,a_3,a_4\}\rightarrow\{-h,-a_3,-a_4\}$. As a consequence, the signs of $a_3$ and $a_4$ are of minor relevance as far as global properties such as the roughness of the surface are concerned.

### B. Physical interpretation of the minimal deposition equation

The second and the third term on the right-hand side (RHS) of Eq. (8) are directly related to the known microscopic mechanisms of (i) the surface diffusion suggested by Mullins [10] and (ii) equilibration of the inhomogeneus concentration of the diffusing particles on the surface as suggested by Villain [3] and Moske [11] (see for alternative argumentation Appendix B). This also implies that the coefficients $a_2$ and $a_3$ are negative. The microscopic origin of the first and the last term on the RHS of Eq. (8), as far as the amorphous surface growth is concerned, does not seem to be available in the literature yet.

Here we propose a simple microscopic argument that leads to *both* terms as a result of *one* dynamical mechanism. Initially, the particles in the beam move in a direction perpendicular to the substrate towards the surface. But when they are close to the surface, they are attracted by interatomic forces in a direction perpendicular to the surface and not perpendicular to the substrate. As a consequence, more particles arrive at places with $\nabla^2h<0$ than at places with $\nabla^2h>0$. This picture is also confirmed by molecular dynamic simulations [13,14] where impinging particles are accelerated towards the surface. For an indication of the relevance of this effect, we refer to the recent experimental study [15]. In a simplified model, the deflection happens instantaneously when a particle arrives at a distance $b$ from the surface where $b$ characterizes the typical range of the interatomic force. Before and after the change of direction the particles move straight, as shown in Fig. 2. This simplification is justified if the kinetic energy of the particles (typically several 0.1 eV for electron beam evaporation) is very small compared to the binding energy on the surface (being typical several eV). Because of this interaction the particles feel an imaginary surface (dashed line in Fig. 2) that is located at a distance $b$ from the real surface, as also shown in Fig. 2. The unit vector perpendicular to the real surface reads

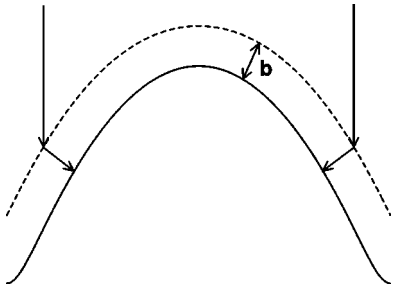


FIG. 2. Sketch of the deflection effect. Particles of the incident beam being perpendicular to the substrate feel at a distance $b$ from the surface (full line) interatomic forces and their trajectories are bent such that they arrive perpendicular to the surface.

$$\vec{n}=\frac{1}{\sqrt{1+(\vec{\nabla}h)^2}}\begin{pmatrix}-\vec{\nabla}h\\ 1\end{pmatrix}. \quad (9)$$

The imaginary surface felt by the particles can be parametrized by

$$\vec{x}'=\vec{x}-\frac{b}{\sqrt{1+(\hat{\nabla}h)^2}}\vec{\nabla}h, \quad (10)$$

$$h'=h+\frac{b}{\sqrt{1+(\vec{\nabla}h)^2}}. \quad (11)$$

Therefore, the number of particles arriving at a place of the real surface (full line in Fig. 2) is increased by a factor

$$\alpha=\det\begin{pmatrix}1-b\partial_x\dfrac{\partial_xh}{\sqrt{1+(\vec{\nabla}h)^2}} & -b\partial_y\dfrac{\partial_xh}{\sqrt{1+(\vec{\nabla}h)^2}}\\ -b\partial_x\dfrac{\partial_yh}{\sqrt{1+(\vec{\nabla}h)^2}} & 1-b\partial_y\dfrac{\partial_yh}{\sqrt{1+(\vec{\nabla}h)^2}}\end{pmatrix}. \quad (12)$$

For small gradients $\vec{\nabla}h$, this factor simplifies to

$$\alpha=\det\begin{pmatrix}1-b\partial_x^2h & -b\partial_y\partial_xh\\ -b\partial_x\partial_yh & 1-b\partial_y^2h\end{pmatrix}=1-b\nabla^2h+b^2M. \quad (13)$$

To obtain the total number of particles arriving at the surface, $\alpha$ has to be multiplied with the mean surface growth $F$,

$$F\alpha = F - Fb\nabla^2 h + Fb^2 M. \tag{14}$$

Since only the deviations from the mean growth $F$ count in the deposition equation (4), the contribution arising from the attraction of the surface to the particles in the growth equation reads

$$-Fb\nabla^2 h + Fb^2 M. \tag{15}$$

Since $b$ is positive, $a_1 = -Fb < 0$ and $a_4 = Fb^2$ holds. The $a_4$ term can be omitted if $b$ is small. As our numerical calculations confirm, the incorporation of small $a_4$ does not qualitatively change the results.

A different expression for the contribution of the particle attraction to the growth of the surface height was derived by Shevchik [16]. His theory should apply well in the limit of large incident velocities of the incoming particles. By contrast, our theory deals with the limit that the kinetic energy of the deposited particles is small before they are attracted by the surface atoms.

In Sec. II, it has been stated that the concentration of the diffusing particles on the surface is given by $n \propto 1/\sqrt{1+(\vec{\nabla}h)^2}$. In the spirit of the aforementioned consideration, this statement must be reexamined. In fact, the number of diffusing particles per surface unit is determined by

$$n \propto \frac{\alpha}{\sqrt{1+(\vec{\nabla}h)^2}} = 1 - b\nabla^2 h - \frac{1}{2}(\vec{\nabla}h)^2 + \mathcal{O}(\nabla^4, h^3). \tag{16}$$

This causes a surface current $\vec{j} \propto -\vec{\nabla} n$ that contributes to the growth equation

$$-\vec{\nabla}\cdot\vec{j} = 2\lambda_1 b\nabla^4 h + \lambda_1 \nabla^2 (\vec{\nabla}h)^2 + \mathcal{O}(\nabla^6, h^3) \tag{17}$$

with $\lambda_1 < 0$. Here, $2\lambda_1 b$ is absorbed into the $a_2$-term. Therefore, the functional form of the growth equation in the small gradient expansion remains unchanged by the fact that the concentration of diffusing particles is $n \propto \alpha/\sqrt{1+(\vec{\nabla}h)^2}$ and not $n \propto 1/\sqrt{1+(\vec{\nabla}h)^2}$.

## IV. STATIONARY SOLUTIONS OF THE DETERMINISTIC FIELD EQUATION

In this section, we investigate the stationary solutions of the deterministic limit of Eq. (4),

$$\partial_t h = a_1\nabla^2 h + a_2\nabla^4 h + a_3\nabla^2(\vec{\nabla}h)^2 \tag{18}$$

on an interval $[0,L]^d$ $(d=1,2)$ subject to periodic boundary conditions. We also discuss their existence and their stability as function of the entering coefficients $a_1$, $a_2$, and $a_3$. To keep the discussion general we allow here for arbitrary signs of the coefficients $a_1$, $a_2$, and $a_3$. Stationary solutions of Eq. (18) are determined by $\partial_t h = 0$ and, therefore, solve $\nabla^2[a_1 h + a_2\nabla^2 h + a_3(\vec{\nabla}h)^2] = 0$. Integrating the latter and using periodic boundary conditions leads to $a_1 h + a_2\nabla^2 h + a_3(\vec{\nabla}h)^2 = \text{const}$. The arbitrary constant that reflects the translational invariance of Eq. (18) in growth direction can be scaled out by the transformation $h \to h - \text{const}/a_1$. Therefore, the stationary solutions of Eq. (18) are determined by

$$a_1 h + a_2\nabla^2 h + a_3(\nabla h)^2 = 0. \tag{19}$$

### A. The solutions

Obviously, Eq. (18) possesses the homogeneous stationary solution $h=0$ for any combination of the coefficients $a_1$, $a_2$, and $a_3$. Due to the nonlinearity $a_3(\vec{\nabla}h)^2$ in Eq. (19), also nonhomogeneous stationary solutions must be expected. If, however, the sign of the ratio of $a_1$ and $a_2$ is negative, then the homogeneous stationary solution $h=0$ is the *only* existing stationary solution. This can be seen as follows. A possible nonhomogeneous stationary solution possesses maxima where $\vec{\nabla}h = 0$ and $\nabla^2 h \leqslant 0$ holds and minima where $\vec{\nabla}h = \vec{0}$ and $\nabla^2 h \geqslant 0$ is satisfied. At the extrema, Eq. (19) reduces to $-(a_1/a_2)h = \nabla^2 h$. This yields the conditions $-(a_1/a_2)h_{\max} \leqslant 0$ at maxima and $-(a_1/a_2)h_{\min} \geqslant 0$ at minima. Necessarily, $h_{\max} > h_{\min}$ must hold. As a consequence, nonhomogeneous stationary solutions cannot exist if $a_1/a_2 < 0$ holds. Here, the sign of $a_3$ is arbitrary.

If the ratio $a_1/a_2$ is positive, spatially varying stationary solutions of Eq. (18) can exist. To understand the appearance of periodic stationary solutions we first consider the case $d=1$ and the fact that Eq. (19) can then be interpreted as the spatial analog of the oscillator with quadratic friction [17]. For $d=1$, Eq. (19) reduces to

$$a_1 h + a_2 h'' + a_3 (h')^2 = 0 \tag{20}$$

with the prime denoting the derivative with respect to the spatial variable. It proves useful to apply the transformation

$$Z = \exp\left(\frac{a_3}{a_2} h\right) \tag{21}$$

to Eq. (20). As a result, one obtains $Z'' + (a_1/a_2) Z \ln Z = 0$ or, equivalently, after integration with respect to the spatial variable

$$\frac{1}{2}Z'^2 + \frac{a_1}{2a_2} Z^2 \left(\ln Z - \frac{1}{2}\right) = \kappa = \text{const}. \tag{22}$$

For positive ratios $a_1/a_2$, the second term on the LHS of Eq. (22) determines a potential $V(Z) = (a_1/2a_2) Z^2 (\ln Z - 1/2)$ and possesses the shape of a well with a minimum at $Z_{\min} = 1$ and $V(Z_{\min}) = -a_1/4a_2$, a local maximum at $Z_{\max} = 0$ and $V(Z_{\max}) = 0$, and diverges proportional $Z^2 \ln Z$ for large $Z$ as depicted in Fig. 3. Only in the interval $-a_1/4a_2 < V(Z) < 0$, the potential possesses two values $Z_1$ and $Z_2$ for the same fixed value of $V(Z)$. Therefore, periodic solutions can only exist if $\kappa$ lies in that interval. The points $Z_1$ and $Z_2$ determine the maximum and minimum values of the height profile $h(x)$. The minimum value of $V(Z)$ at $Z=1$ corresponds to $h(x)=0$. Moreover $\kappa = 0$ corresponds to a height profile $h(x)$ that varies between $h_{\max} = a_2/2a_3$ $(h_{\min} = a_2/2a_3)$ and $h_{\min} = -\infty$ $(h_{\max} = +\infty)$ for $a_2/a_3 > 0$ $(a_2/a_3 < 0)$. In the vicinity of the minimum at $Z=1$, Eq. (22) can be approximated by the *linear* differential equation

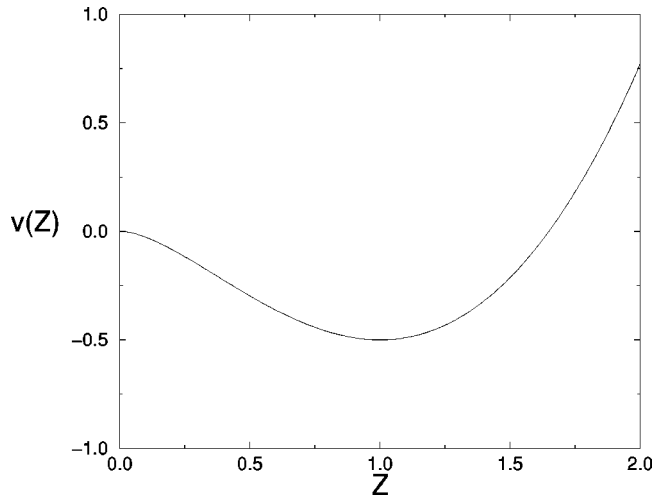


FIG. 3. Dependence of the rescaled potential $v(Z)=2a_2V(Z)/a_1=Z^2(\ln Z-1/2)$ as function of $Z$.

$$Z''+\frac{a_1}{a_2}(Z-1)=0. \tag{23}$$

Therefore, decreasing $\kappa$ to $V(Z_{\min})$, the periodicity length $L$ of the periodic height profile $h(x)$ converges to $2\pi\sqrt{a_2/a_1}$. On the other hand, since $V'(0)=0$, increasing $\kappa$ to zero from below, $L$ increases towards infinity. This implies, however, that periodic solutions of Eq. (20) exist if the condition

$$L>2\pi\sqrt{a_2/a_1} \tag{24}$$

is fulfilled.

The stationary, spatially periodic solution of Eq. (20) can be obtained using the shooting method. The boundary value problem $a_1h+a_2h''+a_3(h')^2=0$ with $h$ being $L$ periodic is transformed to an initial value problem where $h'(0)=0$ is kept fixed and $h(0)$ is varied until $h$ fulfills $h'(L/2)=0$. The fact that only half of the periodicity interval needs to be considered results from the invariance $x\to L-x$ of Eq. (20) in that case. A representative example of the stationary periodic solution for $a_1=a_2=a_3=-1$ is depicted in Fig. 4. Its characteristic and in general nonsinusoidal shape combines a wide mound and a narrow steep well. The larger the periodicity length is, the narrower is the well. Note, however, that the bottom part of the well is not cuspid for finite $L$, but possesses a rounding on a length scale that cannot be resolved in Fig. 4. Therefore, the resulting height profile is still smooth on the periodicity interval.

Next, we determine the dependence of the roughness $w$ of the nonhomogeneous stationary pattern being defined by

$$w^2=\overline{(h-\overline{h})^2} \tag{25}$$

on the length of the interval $L$. As a representative example, we show in Fig. 5 a numerical calculation of $w(L)$ for $2\pi\leqslant L\leqslant 100$ and $a_1=a_2=a_3=-1$ using the shooting method mentioned above. The result can be fitted to

$$w(L)=b_0+b_1L+b_2L^2 \tag{26}$$

with $b_0=-0.121$, $b_1=0.00427$, $b_2=0.0186$. As a consequence, the difference between the minimum and maximum

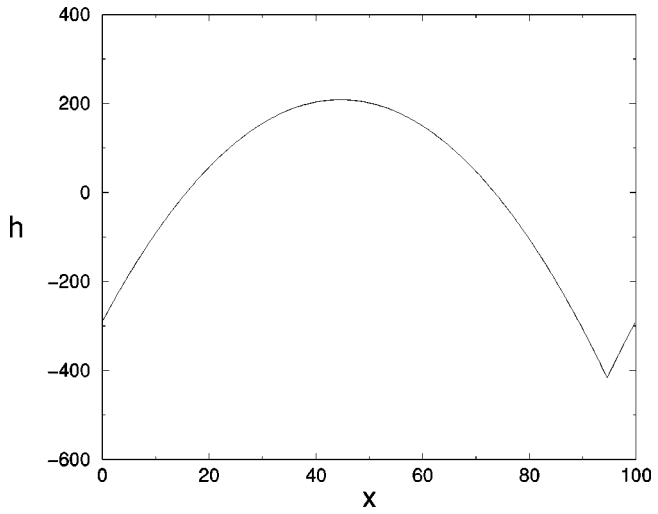


FIG. 4. Stationary solution in 1D: $-h-h''-(h')^2=0$, $L=100$, solved by the shooting method. The height was transformed by $h(x)\to h(x)+\text{const}$ in order to obtain $\int dx\, h(x)=0$. $x$ was transformed by $x\to x+94.6$ in order to shift the minimum of $h(x)$ to $x=94.6$. Thereby coincidence was achieved with the final state of the simulation of the nonlinear deterministic growth equation (36), that is shown in Fig. 6(f).

of the nonhomogeneous stationary solutions scales with $L^2$ for large enough interval length $L$. This can be explained as follows. Shifting the maximum of the nonhomogeneous stationary solutions to $x=0$ and the periodicity interval to $[-L/2,L/2]$, these solutions converge to

$$h(x)=\frac{a_2}{2a_3}-\frac{a_1}{4a_3}x^2 \tag{27}$$

on the interval $[-L/2,L/2]$ for $L\to\infty$. In fact, Eq. (27) is a solution of Eq. (20), but it does not satisfy the periodic boundary conditions on $[-L/2,L/2]$. It corresponds to the case that the constant on the RHS of Eq. (22) is set to zero. The difference between the maximum and minimum of (27) on $[-L/2,L/2]$ is $|a_1L^2/16a_3|$ and its roughness on that interval is determined by

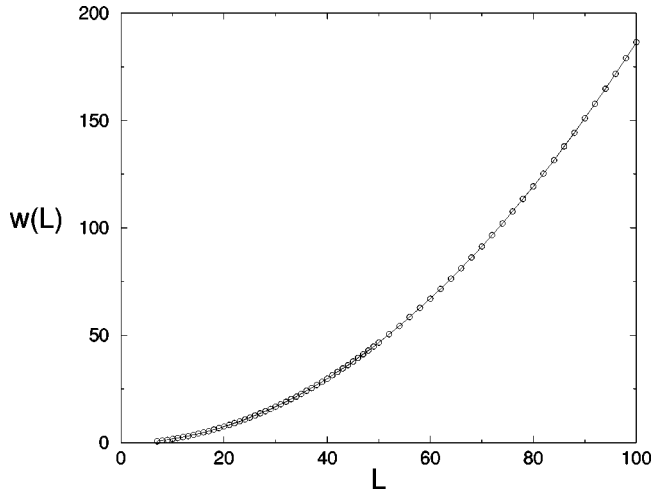


FIG. 5. Surface roughness $w(L)$ of the stationary nonhomogenous solutions as a function of the periodicity interval $L$.

$$w(L)=\frac{1}{8\sqrt{45}}\left|\frac{a_1}{a_3}\right|L^2\approx 0.0186\left|\frac{a_1}{a_3}\right|L^2. \tag{28}$$

This is in perfect agreement with the numerical result, Eq. (26), for large $L$.

The generalization to the two-dimensional case $h(x,y)$ is comparatively simple. Despite the fact that Eq. (19) is nonlinear, it is straightforward to see that an ansatz being an *additive* combination of functions of the different spatial variables $h(x,y)=h_1(x)+h_2(y)$ solves Eq. (19). Moreover, $h_1$ and $h_2$ are directly given by the aforementioned stationary nonhomogeneous solution in the case $d=1$ that exist for $L>2\pi\sqrt{a_2/a_1}$. Due to the rotational invariance in the $x$-$y$ plane (perpendicular to the growth direction), one also infers that even more general solutions of the functional form

$$h(x,y)=h_1\left(\frac{mx+ny}{\sqrt{m^2+n^2}}\right)+h_2\left(\frac{my-nx}{\sqrt{m^2+n^2}}\right) \tag{29}$$

exist where $m$ and $n$ are arbitrary integer numbers and $h_1$ and $h_2$ are given by the stationary solutions in one dimension. In straight analogy to the one-dimensional case, they exist if

$$\frac{L}{\sqrt{m^2+n^2}}>2\pi\sqrt{\frac{a_2}{a_1}} \tag{30}$$

holds since $L/\sqrt{m^2+n^2}$ is the period of $h_1$ and $h_2$ in Eq. (29). Another consequence is that also the squared roughness $w^2$ of the two-dimensional solutions is an *additive* combination of the squares of the roughnesses of the one-dimensional solutions

$$w^2=w_1^2+w_2^2, \tag{31}$$

where $w_i$ is the roughness of $h_i$. As in the one-dimensional case, $w$ scales as $L^2$ for large $L$.

### B. Stability of the solutions

Next, we investigate the stability of the stationary solutions of the deterministic field equation (18). Since the initial state of the growth process is a basically plain surface of the substrate, it is useful to know the conditions for the stability of the homogenous solution $h=0$. These can be obtained by solving the linear limit of Eq. (18)

$$\partial_t h=a_1\nabla^2 h+a_2\nabla^4 h. \tag{32}$$

Using the solution ansatz $h=\exp[i\vec{k}\cdot\vec{x}+\sigma(k)t]$ one obtains the dispersion relation $\sigma(k)=-a_1k^2+a_2k^4$ from Eq. (32).

If $a_2>0$, the growth rate $\sigma(k)$ is positive at least for large enough $k$. Therefore, the homogenous solution is unstable in that case. Furthermore, $\sigma(k)$ increases to infinity for $k\to\infty$. There is no upper limit for the growth rate of Fourier modes with large $k$, and, as an aside, the nonlinearity $a_3\nabla^2(\vec{\nabla}h)^2$ in Eq. (18) makes this worse by doubling the wave vector $\vec{k}$. This implies that for most initial conditions the deterministic field equation (18) has no bounded solution if $a_2$ is positive. Moreover, if $a_2<0$ and $a_1>0$, $\sigma(k)$ is negative for all nonzero $k$, and, therefore, the homogenous stationary solution of Eq. (18) is linearly stable.

The realistic scenario is that $a_1$ and $a_2$ are negative as explained in the previous chapter. In this case, $\sigma(k)$ is positive if $0<k<\sqrt{a_1/a_2}$. The homogenous solution will be unstable if a wave vector $\vec{k}$ exists in that range. Since we investigate Eq. (18) on an interval $[0,L]^d$ subject to periodic boundary conditions, the possible wave vectors are $\vec{k}=(2\pi n_x/L,2\pi n_y/L)$ where $n_x$ and $n_y$ are integer numbers. Therefore, the smallest nonzero $k=|\vec{k}|$ is $k=2\pi/L$. This implies that the homogenous solution is unstable if $2\pi/L<\sqrt{a_1/a_2}$, or equivalently

$$L>2\pi\sqrt{a_2/a_1}. \tag{33}$$

This condition is surely fulfilled in the experiment, because the substrate usually measures about 1 cm in length and width and $2\pi\sqrt{a_2/a_1}$ is only several nm [18]. Therefore, Eq. (33) is a necessary condition for numerical and analytical investigations of Eq. (18) since its neglection would remove the instability of the homogenous solution $h=0$ against the growth of Fourier modes with wave number $k<\sqrt{a_1/a_2}$. The conditions for stability and instability of the homogeneous stationary solution are depicted in Fig. 7.

To investigate the stability of the nonhomogenous stationary solutions of Eq. (18) we solve this equation numerically with $a_1$ and $a_2$ being negative and the assumption that Eq. (33) holds because $a_1/a_2>0$ and Eq. (33) are necessary conditions for the existence of the nonhomogenous stationary solutions. Starting from a random height distribution close to the homogenous solution $h=0$, a periodic surface structure with a wave length of about $\lambda_c=2\pi\sqrt{2a_2/a_1}$ arises and increases in height as depicted in Fig. 6(a). $\lambda_c$ corresponds to the critical wave number $k_c=\sqrt{a_1/2a_2}$ where $\sigma(k)$ has its maximum. At later stages of the evolution, the nonlinearity $a_3\nabla^2(\vec{\nabla}h)^2$ causes a coarsening of the moundlike structure where the mounds grow in length *and* height and the number of mounds decreases. This coarsening precedes in such a way that smaller mounds are ''eaten'' by their bigger neighbors, as shown in Fig. 6. The final state is always a nonhomogenous stationary solution with only *one* mound [see Fig. 6(f)]. In the two-dimensional case, this is the stationary solution $h(x,y)=h_1(x)+h_2(y)$ where $h_1$ and $h_2$ are nonhomogenous stationary solutions in one dimension with the maximum period $L$. We conclude that the nonhomogenous stationary solutions with one mound are stable whereas the nonhomogenous solutions with more than one mound are unstable. The similarity of the results in one and two spatial dimensions is a consequence of the fact that $h(x,y,t)=h_1(x,t)+h_2(y,t)$ is a solution of Eq. (18) in the two-dimensional case if $h_1$ and $h_2$ are solutions of Eq. (18) in the case $d=1$.

If $a_1$ and $a_2$ are positive and Eq. (33) holds, this can be regarded as the result of a time inversion of the case where $a_1$ and $a_2$ are negative. Therefore, the nonhomogenous stationary solutions are unstable. Moreover, for most initial conditions a solution of Eq. (18) does not exist, and numerical simulation is therefore not reasonable in this case. The

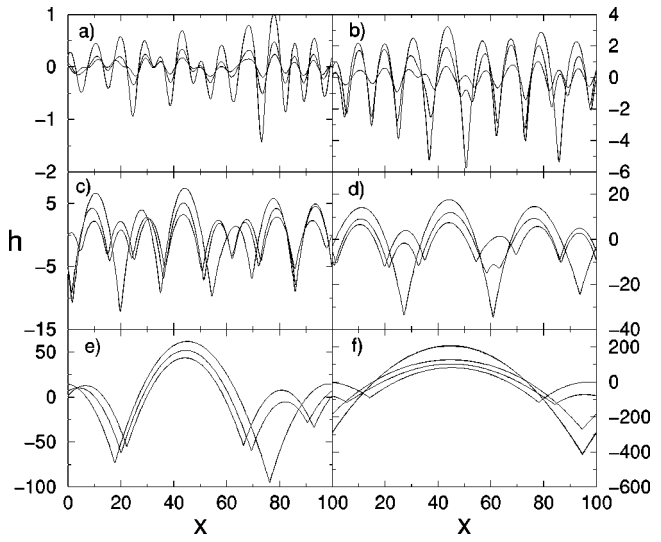


FIG. 6. Height profile $h(x,t)$ calculated from the nonlinear deterministic growth equation in one dimension (36) using the parameters $a_1=a_2=a_3=-1$ on an interval $[0,100]$ subject to periodic boundary conditions. The initial values of $h$ on the 400 grid points are random numbers taken from a uniform distribution between $+0.5$ and $-0.5$. (a) $t=2,6,11$, (b) $t=11,22,33$, (c) $t=33,66,100$, (d) $t=100,150,200$, (e) $t=800,900,1000$, (f) $t=1200,1400,1600,3000,5000,10000$. The height profiles at $t=3000,5000,10\,000$ are coincident with the stationary solution of Eq. (36), that is shown in Fig. 4. The height profiles at different times can be distinguished in such a way that the maximum of $h$ increases with time in the pictures (a)–(f).

conditions for the existence and stability of the nonhomogenous stationary solutions are also depicted in Fig. 7.

## V. QUANTITATIVE INVESTIGATION OF THE MOUND GROWTH

At the end of the last chapter we have described the growth of the moundlike structure arising from the nonlinear deterministic field equation (18) under the conditions that $a_1$ and $a_2$ are both negative. Because these conditions combined with $a_3<0$ are relevant in the context of amorphous surface growth (see Sec. II) we apply them in the rest of this study. Furthermore, we must prevent any artificial effect of the finite size $L$ of the interval $[0,L]^d$ on the surface structure,

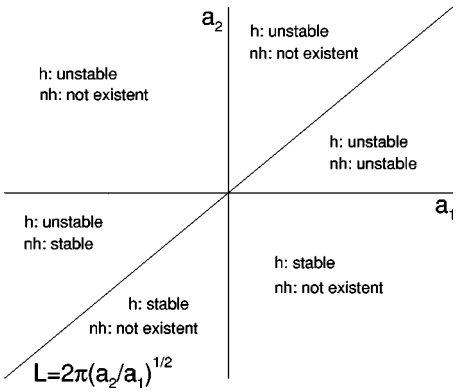


FIG. 7. Stability of the stationary solutions in the parameter space spanned by $a_1$ and $a_2$, h: homogeneous, nh: nonhomogenous.

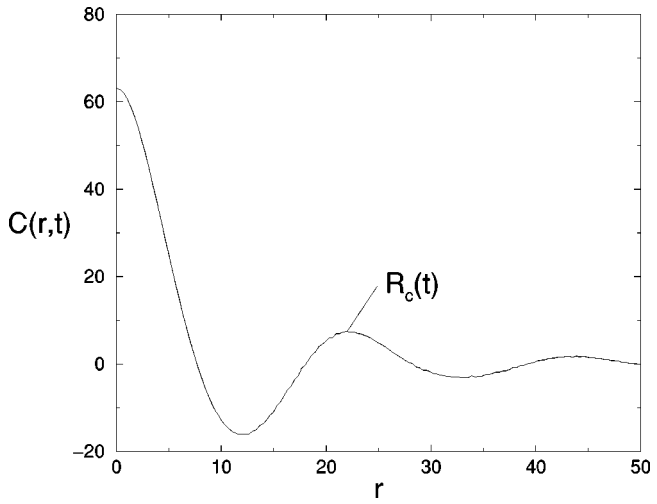


FIG. 8. Height-height correlation $C(r,t)$ at the time $t=100$ resulting from the nonlinear deterministic growth equation (18) in two dimensions on an interval $[0,100]^2$ subject to periodic boundary conditions, using the parameters $a_1=a_2=a_3=-1$. The initial values of $h$ on the $N^2=301^2$ grid points are random numbers taken from a uniform distribution between $+0.5$ and $-0.5$.

because the substrate is usually much larger than the length scale of the observed surface structure [7,8]. Therefore, $L$ must be large compared to the length scale of the calculated surface structure, that is about $\lambda_c=2\pi\sqrt{2a_2/a_1}$ at the beginning of the simulation and is increasing afterwards.

In this section, we first quantitatively investigate the growth of the moundlike structure arising from the nonlinear deterministic growth equation (18) under the aforementioned conditions. Subsequently, we extend our investigation to the nonlinear stochastic field equation (4). For that purpose quantities need to be introduced, that describe the evolution of the height and the length of the surface structure. The height-height-correlation is defined by

$$C(r,t)=\left\langle\left\langle\frac{1}{L^d}\int d^dx[h(\vec{x},t)-\overline{h}(t)]\times[h(\vec{x}+\vec{r},t)-\overline{h}(t)]\right\rangle\right\rangle_{|\vec{r}|=r}, \tag{34}$$

where $\overline{h}(t)=(1/L^d)\int d^dx h(\vec{x},t)$ denotes the spatially average of the height, and $\langle\langle\ldots\rangle\rangle_{|\vec{r}|=r}$ denotes the ensemble and radially average. Then the surface roughness $w(t)$ is given by $w^2(t)=C(0,t)$, and the correlation length $R_c(t)$ is defined as the radius of the first maximum of $C(r,t)$ occuring at nonzero $r$ (see Fig. 8). The quantities $w(t)$ and $R_c(t)$ characterize the height and length of the surface structure. Finally, we define the height-difference correlation by

$$\mathrm{H}(r,t)=\left\langle\left\langle\frac{1}{L^d}\int d^dx(h(\vec{x},t)-h(\vec{x}+\vec{r},t))^2\right\rangle\right\rangle_{|\vec{r}|=r}. \tag{35}$$

$R_c(t)$, $w(t)$, and $H(r,t)$ are experimentally accessible [7] and, therefore, candidates for a comparison of experimental data and theory.

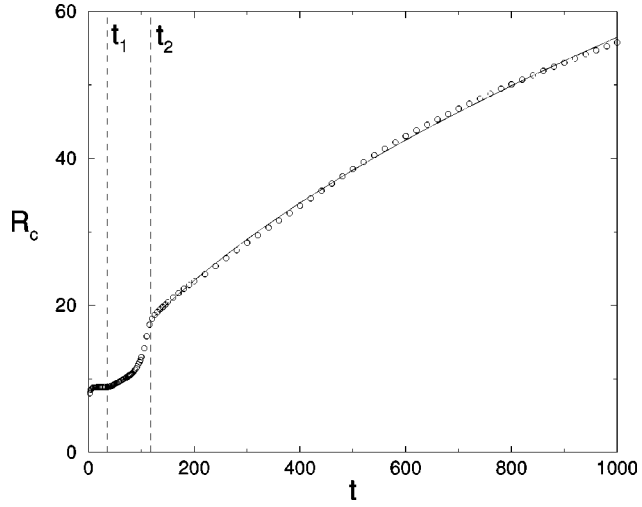


FIG. 9. Correlation length $R_c(t)$ calculated from the nonlinear deterministic growth equation (36) in one dimension using the parameters $a_1=a_2=a_3=-1$ on an interval [0,400] subject to periodic boundary conditions. The initial values of $h$ on the 800 grid points are random numbers taken from a uniform distribution between $+0.0005$ and $-0.0005$. $t_1=34.6$ (left dashed line) denotes the time when $R_c(t)$ climbs over $2\pi\sqrt{2a_2/a_1}$, and $t_2=117.5$ (right dashed line) denotes the time when $R_c(t)$ reaches $4\pi\sqrt{2a_2/a_1}$. The solid line that fits $R_c(t)$ for $t>t_2$ is calculated by $R_c(t)=p_0+\sqrt{p_1+p_2t}$ with the parameters $p_0=-12.4$, $p_1=414.7$, and $p_2=4.3$.

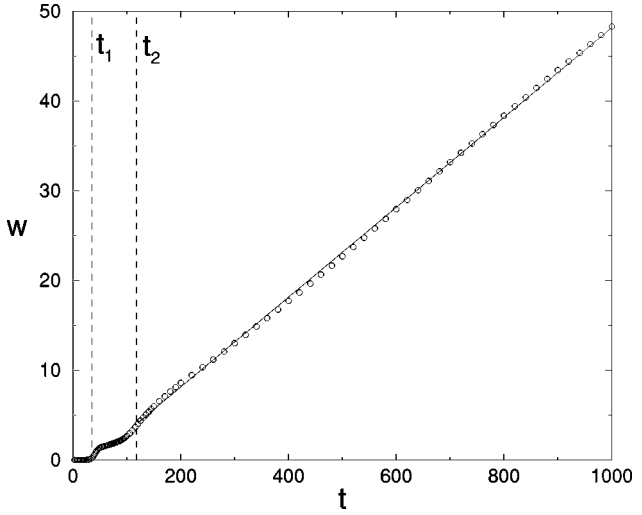


FIG. 10. Surface roughness $w(t)$ resulting from the same simulation as the correlation length in Fig. 9. The solid line that fits $w(t)$ for $t>t_2$ is determined by $w(t)=0.05t+\text{const}$.

### A. Nonlinear deterministic growth equation in one dimension

Here, we investigate the deterministic field equation (18) in the case $d=1$ reading explicitly

$$\partial_t h=a_1\partial_x^2 h+a_2\partial_x^4 h+a_3\partial_x^2(\partial_x h)^2. \tag{36}$$

As a representative example, we solve this equation by numerical simulation (see for details of the method Appendix C) with the coefficients $a_1=a_2=a_3=-1$ and the interval length given by $L=400$. The number of grid points is $N=800$ and the initial values of $h$ on these grid points are independent random numbers taken from a uniform distribution between $+0.0005$ and $-0.0005$. The corresponding results for the correlation length $R_c(t)$ and the surface roughness $w(t)$ are shown in Figs. 9, 10, and 11.

At early stages the linear limit of Eq. (36) $\partial_t h=a_1\partial_x^2 h+a_2\partial_x^4 h$ is sufficient to describe the surface growth. This implies that a Fourier mode with wave number $k$ grows with a growth rate $\sigma(k)=-a_1k^2+a_2k^4$. Because $\sigma(k)$ has its maximum at $k_c=\sqrt{a_1/2a_2}$ and $\sigma(k_c)=-a_1^2/4a_2$, this *critical mode* begins to dominate the surface growth after a short time. Therefore, the correlation length $R_c(t)$ first increases and then remains constant at $R_c(t)=2\pi/k_c=2\pi\sqrt{2a_2/a_1}$ until the time $t=t_1$, when the nonlinearity $a_3\partial_x^2(\partial_x h)^2$ raises $R_c(t)$ above this value (see Fig. 9). For the same reason, the surface roughness $w(t)$ follows approximately a time evolution $\exp[\sigma(k_c)t]=\exp(-a_1^2t/4a_2)$ for $t<t_1$, as soon as the cricital mode begins to dominate the other Fourier modes (see Fig. 11). Actually, the growth of $w(t)$ at $t<t_1$ can be fitted by an $\exp(0.235t)$-behavior (see solid line in Fig. 11) yielding that the growth rate of $w(t)$ is a little bit smaller than $\sigma(k_c)=0.25$. This deviation is caused by the contribution of Fourier modes with growth rate $\sigma(k)<\sigma(k_c)$. We mention that a reduction of the initial values of $h$ would extend the time interval $[0,t_1]$, before the effect of the nonlinear term sets in. Therefore, the critical mode would have more time to dominate the other Fourier modes. This yields that the growth rate of $w(t)$ for $t<t_1$ converges to $\sigma(k_c)$ from below in the limit of very small initial values of $h$.

After $t=t_1$ has been reached, the nonlinear term $a_3\partial_x^2(\partial_x h)^2$ is no longer negligible and is roughly doubling the correlation length $R_c(t)$ in the time interval $[t_1,t_2]$ as shown in Fig. 9 between the dashed lines. Then the curvature of $R_c(t)$ changes and $R_c(t)$ follows asymptotically a $\sqrt{t}$ behavior. The growth of $R_c(t)$ for $t>t_2$ can be fitted by $R_c(t)=p_0+\sqrt{p_1+p_2t}$ with the parameters $p_0=-12.4$, $p_1=414.7$, and $p_2=4.3$ as depicted in Fig. 9 (solid line). The surface roughness $w(t)$ grows linearly beyond $t=t_2$ with the slope $dw/dt=0.05$ as shown in Fig. 10 (solid line).

Next, we investigate the effect of the initial distribution or, equivalently, the initial surface roughness of the height $h$

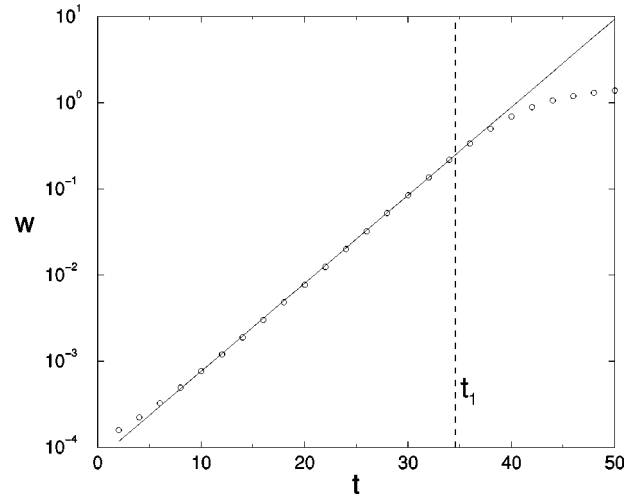


FIG. 11. Surface roughness $w(t)$ resulting from the same simulation as the correlation length in Fig. 9. The solid line that fits $w(t)$ for $t<t_1$ is determined by $w(t)=\text{const}\times\exp(0.235t)$.

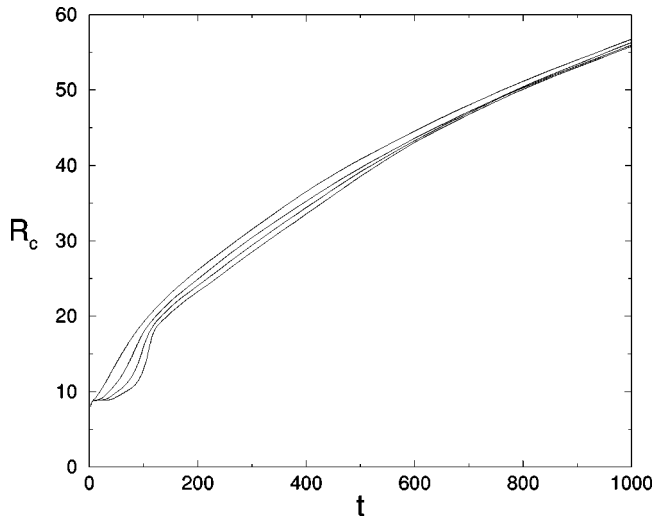


FIG. 12. Correlation length $R_c(t)$ calculated from the nonlinear deterministic growth equation (36) in one dimension using the parameters $a_1=a_2=a_3=-1$ on an interval [0,400] subject to periodic boundary conditions. The initial values of $h$ on the 800 grid points are random numbers taken from uniform distributions between $+0.0005$ and $-0.0005$ (right line), $+0.005$ and $-0.005$ (second line from the right), $+0.05$ and $-0.05$ (third line from the right), and $+0.5$ and $-0.5$ (left line), respectively.

on the growth of $R_c(t)$ and $w(t)$. Again, we solve Eq. (36) on the interval [0,400] with the coefficients $a_1=a_2=a_3=-1$. The initial values of $h$ on the $N=800$ grid points, however, are random numbers taken from four different uniform distributions, namely, between $+0.0005$ and $-0.0005$, $+0.005$ and $-0.005$, $+0.05$ and $-0.05$, and $+0.5$ and $-0.5$. The results for the correlation length $R_c(t)$ and surface roughness $w(t)$ are depicted in Figs. 12 and 13. Figure 12

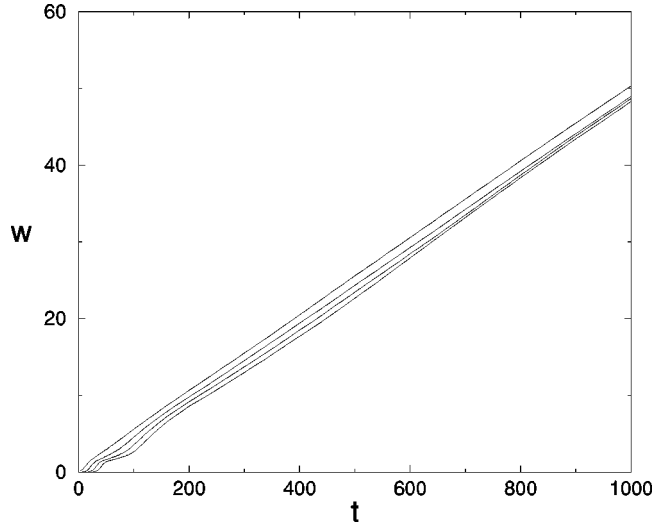


FIG. 13. Surface roughness $w(t)$ calculated from the nonlinear deterministic growth equation (36) in one dimension using the parameters $a_1=a_2=a_3=-1$ on an interval [0,400] subject to periodic boundary conditions. The initial values of $h$ on the 800 grid points are random numbers taken from uniform distributions between $+0.0005$ and $-0.0005$ (right line), $+0.005$ and $-0.005$ (second line from the right), $+0.05$ and $-0.05$ (third line from the right), and $+0.5$ and $-0.5$ (left line), respectively.

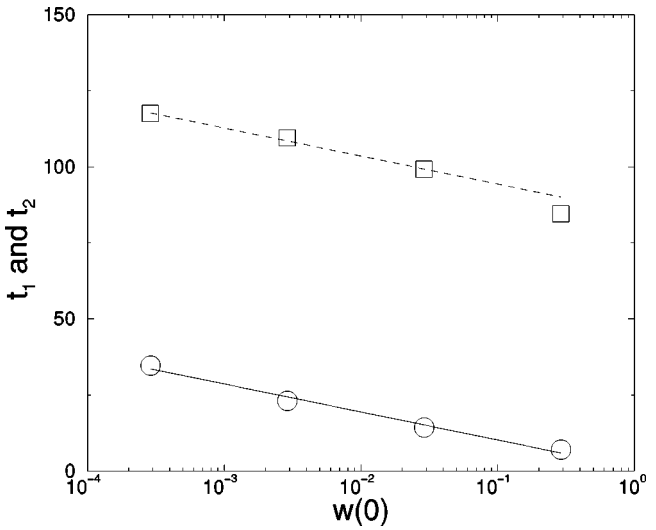


FIG. 14. $t_1$ (circles) and $t_2$ (squares) as functions of the initial surface roughness $w(0)$ calculated from the same simulations as $R_c(t)$ and $w(t)$ in Figs. 12 and 13. The solid line that fits $t_1$ is given by $t_1=-4\ln[w(0)]+1$. The dashed line that fits $t_2$ is given by $t_2=-4\ln[w(0)]+85$.

indicates that the larger the initial values of $h$ are, the smaller is the time $t_1$ when $R_c(t)$ begins to exceed $\lambda_c=2\pi\sqrt{2a_2/a_1}$ and also the time $t_2$ when $R_c(t)$ reaches $2\lambda_c=4\pi\sqrt{2a_2/a_1}$. The dependence of the characteristic times $t_1$ and $t_2$ on the initial surface roughness $w(0)$ is depicted in Fig. 14. As a result, $t_1$ can be approximated by $t_1=-4\ln[w(0)]+1$ or equivalently $w(0)\exp(0.25t_1)=\exp(0.25)=\text{const}$. This implies that the nonlinear term $a_3\partial_x^2(\partial_x h)^2$ begins to take an effect, when the surface roughness $w(t)$, that follows the $w(0)\exp(0.25t)$ behavior for $t<t_1$, comes up to a fixed value. We emphasize that the constant in this law is still dependent on the rescaled initial height distribution $h(x,0)/w(0)$. Furthermore, $t_2$ can be approximated by $t_2=-4\ln[w(0)]+85$, yielding $t_2=t_1+84$. Figures 12 and 13 also indicate that the long time behavior of $R_c(t)$ and $w(t)$, i.e., $R_c(t)\sim\sqrt{t}$ and $w(t)\sim t$ for $t>t_2$, is not influenced by the initial height distribution except that the curves are shifted to later times if the initial values of $h$ are decreased. Another result of Figs. 12 and 13 is that the curves of $R_c(t)$ and $w(t)$ in the transition period $[t_1,t_2]$ are changed from convex into straight, if the initial height $h(x,0)$ increases.

Finally, we extend the discussion of Eq. (36) to general coefficients $a_1$, $a_2$, and $a_3$. We have explained that in the validity regime of the linear equation for $t<t_1$ $R_c(t)$ reaches $\lambda_c=2\pi\sqrt{2a_2/a_1}$ and remains constant until $t=t_1$ and that $w(t)$ follows approximately an $\exp(-a_1^2t/4a_2)$ behavior, as soon as the cricital mode begins to dominate the surface growth.

It is straightforward to see that $-a_2/a_1^2$ is a time constant, $\sqrt{a_2/a_1}$ is a length constant, and $a_2/a_3$ is a height constant in Eq. (36). Changing $a_2/a_3$ by an arbitrary factor would change all heights by the same factor. The same holds for $\sqrt{a_2/a_1}$ and all lengths and $-a_2/a_1^2$ and all times, respectively. Therefore, all relations that hold in the case $a_1=a_2=a_3=-1$ can be generalized by division of all heights by $a_2/a_3$, all lengths by $\sqrt{a_2/a_1}$, and all times by $-a_2/a_1^2$. For

instance $t_1$ is determined by $[a_3 w(0)/a_2]\exp(-0.25a_1^2 t_1/a_2)=\text{const}$ where the constant in this law depends on the function $\hat{h}(x,0)=h(\sqrt{a_1/a_2}x,0)/w(0)$ in the same way as it would depend on $\hat{h}(x,0)=h(x,0)/w(0)$ in the case $a_1=a_2=a_3=-1$. The relation between $t_2$ and $t_1$ can be generalized by $t_2=t_1-84a_2/a_1^2$. These relations yield that, if $|a_3|$ is decreased, $t_2$ and $t_1$ increase. By means of $R_c(t)\sim\sqrt{t}$ one obtains $R_c(t)\sim\text{const}\times\sqrt{a_2/a_1}\sqrt{-a_1^2 t/a_2}=\text{const}\times\sqrt{-a_1 t}$ for $t>t_2$ where the constant does not depend on the coefficients $a_1$, $a_2$, or $a_3$. This seems paradoxical because the coarsening of the surface structure is caused by the nonlinearity $a_3\partial_x^2(\partial_x h)^2$. But, on the other hand, by an increase of $|a_3|$ one could decrease $t_1$ and $t_2$ and shift the $R_c(t)$ curve to smaller times and thereby increase $R_c(t)$ at any fixed time $t>t_2$. Finally, $w(t)$ grows linearly at $t>t_2$ with the slope $dw/dt=0.05(a_2/a_3)(-a_1^2/a_2)=-0.05a_1^2/a_3$.

### B. Nonlinear deterministic growth equation in two dimensions

Next, we investigate the nonlinear deterministic growth equation (8) in the case $d=2$. Except for some quantitative deviations, the same considerations as in one dimension are also valid in two dimensions.

In the regime of the linear growth equation (32) with $t<t_1$, the critical mode with wave number $k_c=\sqrt{a_1/2a_2}$ begins to dominate the other Fourier modes after a short time. Then, the surface roughness $w(t)$ follows again approximately an $\exp[\sigma(k_c)t]=\exp(-a_1^2 t/4a_2)$ behavior and the correlation length remains constant at $R_c(t)=7.0156/k_c=7.0156\sqrt{2a_2/a_1}$. The difference in the behavior of $R_c(t)$ between the case $d=2$ and the case $d=1$ is due to the radially average in the definition of $C(r,t)$.

We solved Eq. (8) on an interval $[0,100]^2$ subject to periodic boundary conditions with the coefficients $a_1=a_2=a_3=-1$ and with $a_4=0$, $a_4=0.08$ and $a_4=0.2$, respectively. The initial values of $h$ on $N^2=301^2$ grid points were random numbers taken from a uniform distribution between $+0.5$ and $-0.5$. The results for $R_c(t)$ and $w(t)$ are depicted in Figs. 15 and 16, respectively. The long time behavior of $R_c(t)$ and $w(t)$ is the same as in the case $d=1$, i.e., $R_c(t)\sim\sqrt{t}$ and $w(t)\sim t$ for $t>t_2$ with the slope of $w(t)$ determined by $dw/dt=0.08$. The deviations from this behavior at later stages are due to the finite size of the interval $[0,100]^2$.

Figures 15 and 16 also indicate that the term proportional to $a_4$ has no *qualitative* effect, except for a little acceleration of the growth of $R_c(t)$ and $w(t)$. Because of the relations $a_4=Fb^2$ and $a_1=-Fb$, $a_4$ is not independent of $a_1$. In a comparison with experimental results [18] we have self-consistently checked that the inclusion of the $a_4$ term does not *quantitatively* impact the results.

The growth behavior of $R_c(t)$ and $w(t)$ at later stages, i.e., $R_c(t)\sim\sqrt{t}$ and $w(t)\sim t$ for $t>t_2$, can be obtained if one applies the transformation $\vec{x}\to b\vec{x}$, $h\to b^\alpha h$, and $t\to b^z t$ to all lengths, heights, and times where $\alpha$ and $z$ are positive constants and $b$ is a positive number. Because the coefficients of Eq. (18) have the dimensions $[a_1]=\text{length}^2/\text{time}$, $[a_2]=\text{length}^4/\text{time}$, and $[a_3]=\text{length}^4/(\text{time}\times\text{height})$, they are transformed thereby according to $a_1\to b^{2-z}a_1$, $a_2\to b^{4-z}a_2$, and $a_3\to b^{4-z-\alpha}a_3$. Then, Eq. (18) is transformed to

$$\partial_t h=b^{2-z}a_1\nabla^2 h+b^{4-z}a_2\nabla^4 h+b^{4-z-\alpha}a_3\nabla^2(\vec{\nabla}h)^2. \tag{37}$$

This equation would correspond to the original Eq. (18) if $2-z=4-z=4-z-\alpha=0$ held. Because this condition cannot be fulfilled, we neglect one of the three terms on the RHS of Eq. (18). We neglect the term proportional to $a_2$ because at large length scales fourth order derivatives are smaller

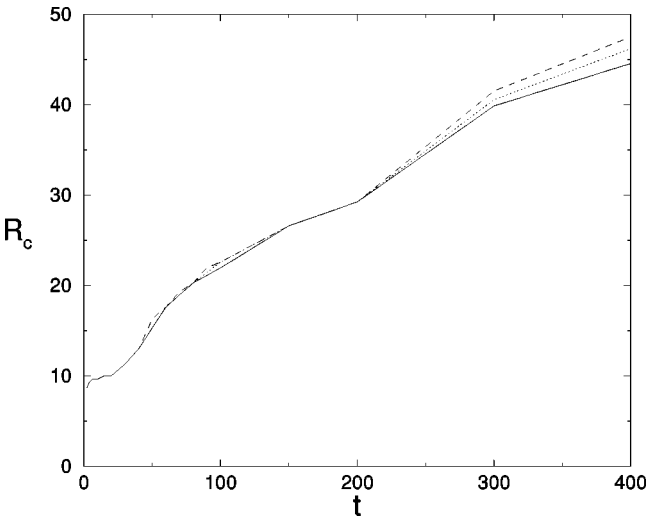


FIG. 15. Correlation length $R_c(t)$ calculated from the nonlinear deterministic growth equation (8) in two dimensions using the parameters $a_1=a_2=a_3=-1$, $a_4=0$ (solid line), $a_4=0.08$ (dotted line), and $a_4=0.2$ (dashed line) on an interval $[0,100]^2$ subject to periodic boundary conditions. The initial values of $h$ on the $N^2=301^2$ grid points are random numbers taken from a uniform distribution between $+0.5$ and $-0.5$.

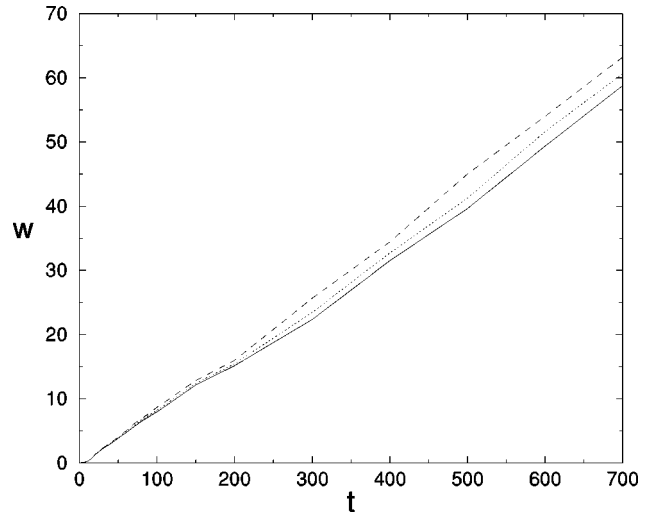


FIG. 16. Surface roughness $w(t)$ calculated from the nonlinear deterministic growth equation (8) in two dimensions using the parameters $a_1=a_2=a_3=-1$, $a_4=0$ (solid line), $a_4=0.08$ (dotted line), and $a_4=0.2$ (dashed line) on an interval $[0,100]^2$ subject to periodic boundary conditions. The initial values of $h$ on the $N^2=301^2$ grid points are random numbers taken from a uniform distribution between $+0.5$ and $-0.5$.

than second order derivatives and at large heights linear terms are smaller than quadratic terms. So $a_2\nabla^4 h$ is small compared to $a_1\nabla^2 h$ and $a_3\nabla^2(\vec{\nabla}h)^2$. Therefore, we can omit the condition $4-z=0$ and we retain the conditions $2-z=4-z-\alpha=0$, yielding $z=\alpha=2$. Then one obtains that $R_c(t)$ follows a time evolution determined by $R_c(t)\sim t^{1/z}=t^{1/2}$, $w(t)$ follows a dynamics given directly by $w(t)\sim t^{\alpha/z}=t$, and the surface roughness of the stationary solutions of Eq. (18) is governed by $w(L)\sim L^{\alpha}=L^2$. Furthermore, the height-difference correlation can be written as $H(r,t)=r^{2\alpha}g(t/r^z)=r^4 g(t/r^2)$ for $t>t_2$, as we confirmed by numerical simulations of the deterministic growth equation (18). This, however, does *not* imply that $H(r,t)$ follows a $r^4$ behavior at a fixed time $t>t_2$ and small $r$, because $g(\xi)$ does *not* saturate for large $\xi=t/r^2$.

### C. Linear stochastic growth equation

As a first approach to obtain insights in the dynamics of the nonlinear stochastic growth equation (4), we investigate its linear limit

$$\partial_t h=a_1\nabla^2 h+a_2\nabla^4 h+\eta \tag{38}$$

on an interval $[0,L]^d$ subject to periodic boundary condition and the initial condition $h(\vec{x},0)=0$. Equation (38) has proved to be sufficient to describe the surface growth of amorphous ZrAlCu films up to a layer thickness of about $\langle H\rangle=240$ nm [18]. The height-height correlation $C(r,t)$ that arises from this equation is determined by

$$C(r,t)=\left\langle \frac{D}{L^d}\sum_{\vec{k}\neq 0}\exp(i\vec{k}\cdot\vec{r})\frac{\exp[2\sigma(k)t]-1}{\sigma(k)}\right\rangle_{|\vec{r}|=r}, \tag{39}$$

where $\langle\cdots\rangle_{|\vec{r}|=r}$ denotes radially average and $\sigma(k)=-a_1k^2+a_2k^4$ the growth rate of the Fourier modes. Since all possible wave vectors $\vec{k}$ have the form $\vec{k}=(2\pi n_x/L,2\pi n_y/L)$, where $n_x$ and $n_y$ are integer numbers, $C(r,t)$ converges in the limit of large $L$, yielding

$$C(r,t)=\left\langle \frac{D}{(2\pi)^d}\int d^dk\,\exp(i\vec{k}\cdot\vec{r})\frac{\exp[2\sigma(k)t]-1}{\sigma(k)}\right\rangle_{|\vec{r}|=r}. \tag{40}$$

Therefore, the RHS of Eq. (39) is basically independent of $L$.

Next, we investigate the scaling behavior of the surface growth arising from Eq. (38) at early stages. If $t>0$ is small compared to $-a_2/a_1^2$, the wave number $k$ must be large compared to $\sqrt{a_1/a_2}$ if a noticeable difference between the term $\{\exp[2\sigma(k)t]-1\}/\sigma(k)$ in Eq. (39) and $2t$ should appear. Therefore, $C(r,t)$ varies on a length scale that is much smaller than $\sqrt{a_2/a_1}$. On that length scale, the term proportional to $a_1$ in Eq. (38) can be neglected yielding $\partial_t h=a_2\nabla^4 h+\eta$. If one applies the transformation $\vec{x}\to b\vec{x}$, $h\to b^{\alpha}h$, and $t\to b^z t$, the coefficients of this equation are changed by $a_2\to b^{4-z}a_2$ and $D\to b^{2\alpha+d-z}D$. This implies that the equation is not changed if the condition $4-z=2\alpha+d-z=0$ holds. This yields $z=4$ and $\alpha=(4-d)/2$. Therefore, $R_c(t)$ follows a $t^{1/z}=t^{1/4}$ behavior and $w(t)$ follows a $t^{\alpha/z}=t^{(4-d)/8}$ behavior if $t$ is small compared to $-a_2/a_1^2$.

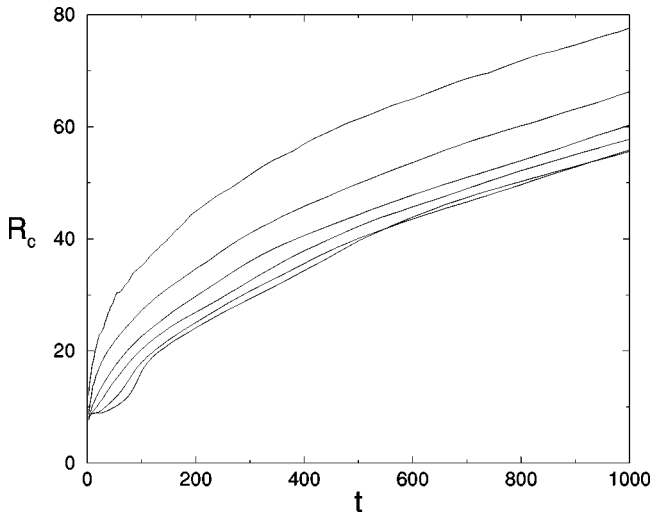


FIG. 17. Correlation length $R_c(t)$ resulting from the nonlinear stochastic growth equation (41) in one dimension on an interval [0,400] subject to periodic boundary conditions, using the parameters $a_1=a_2=a_3=-1$ and $D=10^1,10^0,10^{-1},10^{-2},10^{-4},10^{-6}$ (from the left line to the right line), respectively.

At later stages, the critical mode dominates the surface growth. Then the surface roughness $w(t)$ follows an $\exp(-a_1^2t/4a_2)$ law and the correlation length $R_c(t)$ saturates into $R_c(t)=2\pi\sqrt{2a_2/a_1}$ in the case $d=1$ and into $R_c(t)=7.0156\sqrt{2a_2/a_1}$ in the case $d=2$.

### D. Nonlinear stochastic growth equation in one dimension

In this section, we discuss the nonlinear stochastic growth equation (4) in the case $d=1$:

$$\partial_t h=a_1\partial_x^2 h+a_2\partial_x^4 h+a_3\partial_x^2(\partial_x h)^2+\eta. \tag{41}$$

For this, we solve Eq. (41) on an interval [0,400] subject to periodic boundary conditions and the initial condition $h(x,0)=0$, using the parameters $a_1=a_2=a_3=-1$ and $D=10^1,10^0,10^{-1},10^{-2},10^{-4},10^{-6}$, respectively. Figures 17 and 18 depict the corresponding correlation length $R_c(t)$ and surface roughness $w(t)$.

At early stages the linear growth equation (38) is sufficient to describe the surface growth. Then the height $h$ of the surface profile is proportional to $\sqrt{D}$ whereas the length scale of the surface structure does not depend on $D$. If the noise strength $D$ is small, it takes longer time, before the nonlinear term $a_3\partial_x^2(\partial_x h)^2$ gains an effect. Then, the critical mode has enough time to dominate the other Fourier modes. Therefore, $w(t)$ follows an $\exp(-a_1^2t/a_2)$ behavior and $R_c(t)$ remains constant at $R_c(t)=2\pi\sqrt{2a_2/a_1}$ until the time $t=t_1$, when $R_c(t)$ begins to exceed this value by the effect of the nonlinear term. On the other hand, for large $D$ this behavior is not seen, because the critical mode has not enough time to dominate the other modes before the effect of the nonlinear term sets in.

Figures 17 and 18 also indicate that the growth of the correlation length $R_c(t)$ and the surface roughness $w(t)$ at later stages is not changed by the stochastic term if $D$ is

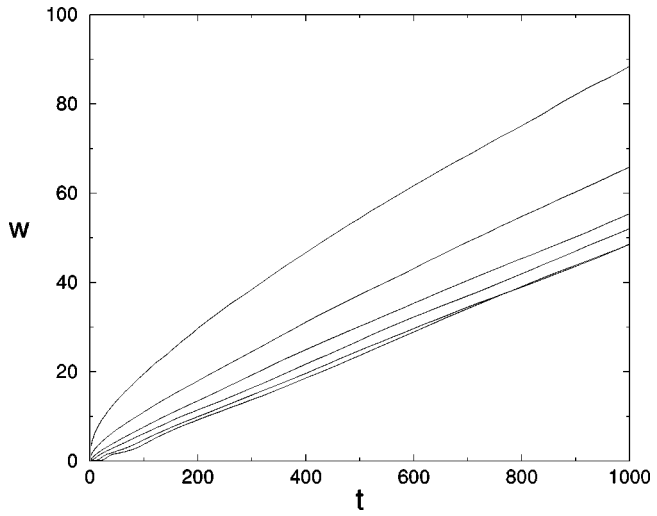


FIG. 18. Surface roughness $w(t)$ resulting from the nonlinear stochastic growth equation (41) in one dimension on an interval $[0,400]$ subject to periodic boundary conditions, using the parameters $a_1=a_2=a_3=-1$ and $D=10^1,10^0,10^{-1},10^{-2},10^{-4},10^{-6}$ (from the left line to the right line), respectively.

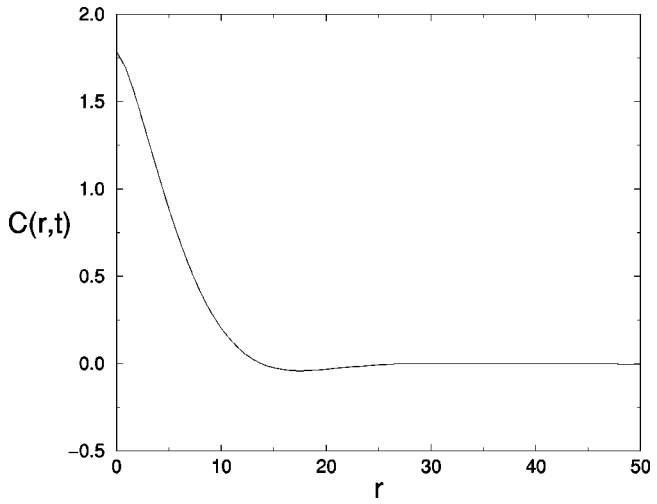


FIG. 19. Height-height correlation $C(r,t)$ at the time $t=100$ resulting from the nonlinear stochastic growth equation (42) in two dimensions on an interval $[0,300]^2$ subject to periodic boundary conditions, using the parameters $a_2=a_3=-1$ and $D=1$.

small, i.e., $R_c(t)$ still follows a $\sqrt{t}$ law and $w(t)$ grows linearly for $t>t_2$ with the slope $dw/dt=-0.05a_1^2/a_3$. This is a consequence of the fact that the stochastic term is not increasing whereas the magnitude of the moundlike surface structure is increasing. Therefore, we expect the same long-time behavior also for large noise strength $D$ at later stages of the surface growth.

### E. Nonlinear stochastic growth equation with $a_1=0$

To ascertain the relevance of the growth instability determined by the term $a_1\nabla^2 h$ (with $a_1<0$) for the growth of a periodic moundlike structure, we investigate the case when it is absent. Thus, we discuss Eq. (4) in the limit $a_1=0$:

$$\partial_t h=a_2\nabla^4 h+a_3\nabla^2(\vec{\nabla}h)^2+\eta, \tag{42}$$

where $a_2$ and $a_3$ are negative numbers. This equation (with $a_3>0$) was proposed by Lai and Das Sarma [5] as the relevant growth equation for *ideal* MBE growth of crystalline layers at higher temperatures. They stated that the surface arising from Eq. (42) evolves into a self-similar structure and they derived the growth exponents $\alpha=(4-d)/3$, $z=(8+d)/3$, and $\beta=\alpha/z=(4-d)/(8+d)$ from a dynamic renormalization-group analysis.

These exponents describe the scaling behavior of Eq. (42) at later stages and large distances. At early stages and small distances the dynamic exponents resulting from the linear limit of Eq. (42) are valid: $\alpha=(4-d)/2$, $z=4$ and $\beta=\alpha/z=(4-d)/8$. By a numerical calculation of the height-height correlation $C(r,t)$ corresponding to Eq. (42) we have confirmed that no periodic structures arise. Therefore, $C(r,t)$ possesses no maximum at nonzero $r$ (see Fig. 19) and the correlation length $R_c(t)$ is not defined.

We conclude that the incorporation of the growth instability induced by the term $a_1\nabla^2 h$ is necessary to describe the experimentally observed formation of a mesoscopic moundlike structure of the growth of amorphous thin films.

## VI. CONCLUSIONS

In this study, we have proposed a nonlinear stochastic field equation (4) for amorphous thin film growth. Starting from a phenomenological approach based on nonlinear stochastic partial differential equations, using the symmetry principles relevant for amorphous film growth, the condition of no excess velocity, and an expansion in the gradients of the surface profile $h(\vec{x},t)$ we obtained the functional form of the equation. Furthermore, we related the constituents of the growth equation to processes determining the interaction of the depositing particles with the already condensed surface atoms. Most importantly, we have demonstrated that the one-dimensional and deterministic limit of Eq. (4) already contains many major ingredients for the understanding of the two-dimensional and/or stochastic case. In particular, the growing surface morphology typically possesses a periodic moundlike structure that coarsens with increasing time, i.e., with increasing time mounds successively disappear and the moundlike structure widens. In the nonlinear regime the characteristic length scale of the surface structure follows a $\sqrt{t}$ behavior whereas its typical height grows linearly with time $t$.

The condition of no excess velocity implies that the film growth occurs at constant density. On the other hand, the possibility of density variations at amorphous film growth cannot be rejected by physical arguments. Furthermore, a comparison of experimental results for amorphous ZrAlCu films indicates the necessity of incorporating density variations [18] at least for that material. Therefore, it is important as a next step to extend our analysis of the growth equation for the case of a basically homogeneous density (4) to a thorough investigation of the long-time behavior of the growth equation in the presence of significant density variations (D4).

## ACKNOWLEDGMENTS

This work has been supported by the DFG-Sonderforschungsbereich 438 München/Augsburg, TP A1.

We thank M. Moske, S. G. Mayr, and K. Samwer for useful discussions.

## APPENDIX A

In this chapter, we discuss the role of the deposition noise by means of statistical considerations. We also present an estimation of the noise strength $D$ in microscopic terms.

If $n$ undistinguishable particles arrive on the surface within a time and space interval of the size $(\Delta x)^2\Delta t$, the number of distributions of the $n$ particles within that time, and space interval scales such as $[(\Delta x)^2\Delta t]^n/n!$. This implies that, if $N$ particles arrive on the total surface area $L^2$ within the time interval $[0,T]$, the probability that $n$ of the particles arrive on a surface area $(\Delta x)^2$ within a time interval of the length $\Delta t$, is given by

$$P(n)=\frac{N!}{n!(N-n)!}\left(\frac{(\Delta x)^2\Delta t}{L^2T}\right)^n\left(1-\frac{(\Delta x)^2\Delta t}{L^2T}\right)^{N-n}. \tag{A1}$$

The total number of deposited particles is given by $N=\Phi_0L^2T$ where $\Phi_0$ is the number of deposited particles per surface area and time. Therefore, the probability $P(n)$ reads

$$P(n)=\frac{N!}{n!(N-n)!}\left(\frac{\Phi_0(\Delta x)^2\Delta t}{N}\right)^n\left(1-\frac{\Phi_0(\Delta x)^2\Delta t}{N}\right)^{N-n}. \tag{A2}$$

Because of $\Phi_0(\Delta x)^2\Delta t\ll\Phi_0L^2T=N$, one obtains $n\ll N$, yielding

$$P(n)=\frac{1}{n!}[\Phi_0(\Delta x)^2\Delta t]^n\exp[-\Phi_0(\Delta x)^2\Delta t]. \tag{A3}$$

Equation (A3) constitutes the Poisson distribution. It has the mean $\langle n\rangle=\Phi_0(\Delta x)^2\Delta t$ and the variance $\langle(n-\langle n\rangle)^2\rangle=\Phi_0(\Delta x)^2\Delta t$. The spatially averaged height increase $\overline{\Delta H}$ that is caused on a surface area $(\Delta x)^2$ by the deposition of $n$ particles of the volume $\Omega$ during a time interval $\Delta t$ reads $\overline{\Delta H}=n\Omega/(\Delta x)^2$. It possesses the mean $\langle\overline{\Delta H}\rangle=\langle n\rangle\Omega/(\Delta x)^2=\Phi_0\Omega\Delta t=F\Delta t$ and, therefore, the variance

$$\begin{aligned}\langle(\overline{\Delta H}-\langle\overline{\Delta H}\rangle)^2\rangle&=\langle(n-\langle n\rangle)^2\rangle\Omega^2/(\Delta x)^4\\&=\Phi_0\Omega^2\Delta t/(\Delta x)^2=F\Omega\Delta t/(\Delta x)^2.\end{aligned} \tag{A4}$$

On the other hand, the height increase produced by deposition reads

$$\overline{\Delta H}=F\Delta t+\frac{1}{(\Delta x)^2}\int_t^{t+\Delta t}\int_{(\Delta x)^2}\eta(\vec{x},t)d^2x\,dt \tag{A5}$$

yielding $\langle\overline{\Delta H}\rangle=F\Delta t$ and finally

$$\langle(\overline{\Delta H}-\langle\overline{\Delta H}\rangle)^2\rangle=2D\Delta t/(\Delta x)^2. \tag{A6}$$

By a comparison of Eqs. (A4) and (A6) one obtains the relation

$$2D=F\Omega \tag{A7}$$

for the noise strength where $F$ is the mean surface growth and $\Omega$ is the particle volume.

## APPENDIX B

Here, we present a derivation of the nonlinear term $a_3\nabla^2(\vec{\nabla}h)^2$ in Eq. (8) that is a modification of the argument in Ref. [11]. It allows for an estimation of the size of the coefficient $a_3$ in microscopic terms and also the determination of its sign. The flux of incoming particles per surface area and time unit generally depends on the slope of the surface

$$\Phi(\vec{y})=\Phi_0/\sqrt{1+(\vec{\nabla}h)^2}\approx\Phi_0\left(1-\frac{1}{2}(\vec{\nabla}h)^2\right). \tag{B1}$$

A particle that arrives at the location $\vec{y}$ diffuses along the surface until it relaxes at the location $\vec{x}$ with probability $d^2x\,P(|\vec{x}-\vec{y}|)$. Here, $\vec{x}$ and $\vec{y}$ are coordinates in the local system of the surface. The mean square of the diffusion length is defined by $l^2=\int d^2x(\vec{x}-\vec{y})^2P(|\vec{x}-\vec{y}|)$. The number of particles that relax at $\vec{x}$ per surface area and time unit is therefore given by

$$\int d^2y\,\Phi(\vec{y})P(|\vec{x}-\vec{y}|)=\Phi(\vec{x})+\frac{1}{4}l^2\nabla^2\Phi|_{\vec{x}}+\mathcal{O}(l^4). \tag{B2}$$

The product of this quantity with $\Omega\sqrt{1+(\vec{\nabla}h)^2}$ determines the growth velocity in growth direction where $\Omega=F/\Phi_0$ is the particle volume. Therefore, the growth velocity reads

$$F-\frac{1}{8}Fl^2\nabla^2(\vec{\nabla}h)^2+\mathcal{O}(l^4), \tag{B3}$$

in the case of small gradients and small diffusion length $l$. As a consequence, the spatial deviation of the growth velocity from the mean growth velocity $F$ being the relevant term entering in the gradient expansion of Eq. (8) is basically determined by the second term in Eq. (B3),

$$a_3=-\frac{1}{8}Fl^2 \tag{B4}$$

with $a_3$ being negative.

An alternative derivation of the coefficient $a_3$ is explained as follows. Because of a geometrical reason [11] the concentration of diffusing particles on the surface is given by $n=n_0/\sqrt{1+(\vec{\nabla}h)^2}$ with $n_0=\Phi_0\tau=\Phi_0l^2/4D'$. Here, $\tau$ is the mean time of particle diffusion before relaxation, and $D'$ is the diffusion constant of the particles on the surface. Unlike this, the adatom density on *crystalline* layers is slope dependent because of the capture of particles at steps. A useful interpolation formula in that connection is $n=n_0/[1+l^2(\vec{\nabla}h)^2/a_\perp^2]$ where $a_\perp$ is the thickness of one atomic layer [19]. The inhomogeneous particle concentration leads to a diffusion current $\vec{j}=-D'\vec{\nabla}n$ and therefore to a contribution $\Omega D'\nabla^2n$ to the deposition equation. This contribution to the deposition equation reads

$$\frac{Fl^2}{4}\nabla^2\frac{1}{\sqrt{1+(\vec{\nabla}h)^2}}\approx-\frac{Fl^2}{8}\nabla^2(\vec{\nabla}h)^2 \tag{B5}$$

at amorphous film growth and

$$\frac{Fl^2}{4}\nabla^2\frac{1}{1+l^2(\vec{\nabla}h)^2/a_\perp^2}\approx-\frac{Fl^4}{4a_\perp^2}\nabla^2(\vec{\nabla}h)^2 \tag{B6}$$

at the growth of crystalline layers [19] and shows most clearly the difference between amorphous and crystalline growth processes.

## APPENDIX C

To integrate numerically the growth equation (4), a forward-backward difference method on a quadratic lattice combined with a Euler algorithm in time has been used [20]. In discrete form, Eq. (4) can be rewritten as

$$h_{i,j}^{n+1}=h_{i,j}^n+\frac{\Delta t_n}{(\Delta x)^2}[w_{i+1,j}^n+w_{i-1,j}^n+w_{i,j+1}^n+w_{i,j-1}^n-4w_{i,j}^n]+\sqrt{\frac{24D\Delta t_n}{(\Delta x)^2}}r_{i,j}^n, \tag{C1}$$

$$\begin{aligned}w_{i,j}^n=a_1h_{i,j}^n&+\frac{a_2}{(\Delta x)^2}[h_{i+1,j}^n+h_{i-1,j}^n+h_{i,j+1}^n+h_{i,j-1}^n-4h_{i,j}^n]\\&+\frac{a_3}{3(\Delta x)^2}[(h_{i+1,j}^n-h_{i,j}^n)^2\\&+(h_{i+1,j}^n-h_{i,j}^n)(h_{i,j}^n-h_{i-1,j}^n)+(h_{i,j}^n-h_{i-1,j}^n)^2\\&+(h_{i,j+1}^n-h_{i,j}^n)^2+(h_{i,j+1}^n-h_{i,j}^n)(h_{i,j}^n-h_{i,j-1}^n)\\&+(h_{i,j}^n-h_{i,j-1}^n)^2],\end{aligned} \tag{C2}$$

where $h_{i,j}^n$ denotes $h(x_i,y_j,t_n)$ and every $r_{i,j}^n$ is an independent random number taken from a uniform distribution between $-1/2$ and $1/2$. The prefactor $\sqrt{24D\Delta t_n/(\Delta x)^2}$ guarantees that the noise $\sqrt{24D\Delta t_n/(\Delta x)^2}r_{i,j}^n$ has the same variance as the spatial average of the Gaussian noise $\eta$ on the quadratic area $(\Delta x)^2$ around $(x_i,y_j)$ integrated over the time interval $[t_n,t_n+\Delta t_n]$:

$$\sqrt{24D\Delta t_n/(\Delta x)^2}r_{i,j}^n=\frac{1}{(\Delta x)^2}\int_{t_n}^{t_n+\Delta t_n}dt\int_{x_i-\Delta x/2}^{x_i+\Delta x/2}dx\int_{y_j-\Delta x/2}^{y_j+\Delta x/2}dy\,\eta(x,y,t). \tag{C3}$$

Equation (C3) means only that its two sides have the same mean and variance. During the simulation the time increment $\Delta t_n=t_{n+1}-t_n$ has been dynamically adjusted.

## APPENDIX D

In Sec. III we derived the simplest nonlinear growth equation using the symmetries relevant for amorphous film growth, the condition of no excess velocity and a low-order expansion in the gradients of the height profile $h(\vec{x},t)$: $\partial_t h=a_1\nabla^2h+a_2\nabla^4h+a_3\nabla^2(\vec{\nabla}h)^2+a_4M+\eta$, yielding $\partial_t H=a_1\nabla^2H+a_2\nabla^4H+a_3\nabla^2(\vec{\nabla}H)^2+a_4M+F+\eta$. If the film grows at contant density $\rho_0$, the number of atoms of the amorphous film per substrate area above a given substrate position reads $c=\rho_0H$, yielding

$$\partial_t c=\rho_0[a_1\nabla^2H+a_2\nabla^4H+a_3\nabla^2(\vec{\nabla}H)^2+a_4M+F+\eta]. \tag{D1}$$

If significant density variations occur during the growth process, the condition of no excess velocity is no more justified even if all deposited particles contribute to the film growth, i.e., if desorption is absent. If the density of the amorphously grown material depends on the surface slope, $\rho=\rho(\vec{\nabla}H)$, $\partial_t c=\rho(\vec{\nabla}H)\partial_t H$ holds instead of $c=\rho_0H$. Here $\rho(\vec{\nabla}H)$ denotes the density at the surface. On the other hand, Eq. (D1) still holds since the absence of particle desorption implies that the rate of change of $c$ is given by a continuity equation $\partial_t c=\rho_0[-\vec{\nabla}\cdot\vec{j}+F+\eta]$. Division of Eq. (D1) by $\rho(\vec{\nabla}H)$ leads to

$$\partial_t H=\frac{\rho_0}{\rho(\vec{\nabla}H)}[a_1\nabla^2H+a_2\nabla^4H+a_3\nabla^2(\vec{\nabla}H)^2+a_4M+F+\eta]. \tag{D2}$$

Next we expand $\rho_0/\rho(\vec{\nabla}H)$ in terms of the gradients $\vec{\nabla}H$: $\rho_0/\rho(\vec{\nabla}H)=1+(a_5/F)(\vec{\nabla}H)^2+\mathcal{O}[(\vec{\nabla}H)^4]$. Then, the expansion of the deterministic part of the RHS of Eq. (D2) up to the order $\mathcal{O}(\nabla^4,H^2)$ and neglecting all corrections to the deposition noise yields

$$\partial_t H=a_1\nabla^2H+a_2\nabla^4H+a_3\nabla^2(\vec{\nabla}H)^2+a_4M+a_5(\nabla H)^2+F+\eta. \tag{D3}$$

Finally, by the transformation $h(\vec{x},t)=H(\vec{x},t)-Ft$, one obtains

$$\partial_t h=a_1\nabla^2h+a_2\nabla^4h+a_3\nabla^2(\vec{\nabla}h)^2+a_4M+a_5(\vec{\nabla}h)^2+\eta \tag{D4}$$

as the relevant continuum model for amorphous film growth in the presence of local density variations depending on the surface slope. The fifth term on the RHS of Eq. (D4) is of Kardar-Parisi-Zhang (KPZ) form [12] and leads to a finite excess velocity. Note that $a_5$ must be positive, because at oblique particle incidence exposed atoms cast a shadow upon unoccupied places on the surface and thereby cause an additional volume increase if the surface diffusion is weak. A comparison with experimental results on amorphous $Zr_{65}Al_{7.5}Cu_{27.5}$-film growth [18] ascertains that Eq. (D4) constitutes a valid model for amorphous thin film growth.

[1] A. L. Barabasi and H. E. Stanley, *Fractal Concepts in Surface Growth* (Cambridge University Press, Cambridge, England, 1995); W. M. Tong and R. S. Williams, Annu. Rev. Phys. Chem. **45**, 401 (1994); J. Krug, Adv. Phys. **46**, 139 (1997); M. Marsili, A. Maritan, F. Toigo, and J. R. Banavar, Rev. Mod. Phys. **68**, 963 (1996).
[2] D. E. Wolf and J. Villain, Europhys. Lett. **13**, 389 (1990).
[3] J. Villain, J. Phys. I **1**, 19 (1991).
[4] S. Das Sarma and P. Tamborenea, Phys. Rev. Lett. **66**, 325 (1991).
[5] Z.-W. Lai and S. Das Sarma, Phys. Rev. Lett. **66**, 2348 (1991).
[6] M. Siegert and M. Plischke, Phys. Rev. E **50**, 917 (1994).
[7] B. Reinker, M. Moske, and K. Samwer, Phys. Rev. B **56**, 9887 (1997); S. G. Mayr, M. Moske, and K. Samwer, Europhys. Lett. **44**, 465 (1998); S. G. Mayr, M. Moske, and K. Samwer, Phys. Rev. B **60**, 16 950 (1999).
[8] T. Salditt, T. H. Metzger, J. Peisl, B. Reinker, M. Moske, and K. Samwer, Europhys. Lett. **32**, 331 (1995).
[9] S. F. Edwards and D. R. Wilkinson, Proc. R. Soc. London, Ser. A **381**, 17 (1982).
[10] W. W. Mullins, J. Appl. Phys. **28**, 333 (1957).
[11] M. Moske, *Mechanische Spannungen als Sonde für Schichtwachstum und Schichtreaktionen* (Habilitationsschrift, Universität Augsburg, 1997).
[12] M. Kardar, G. Parisi, and Y.-C. Zhang, Phys. Rev. Lett. **56**, 889 (1986).
[13] W. D. Luedtke and U. Landman, Phys. Rev. B **40**, 11 733 (1989).
[14] G. De Lorenzi and G. Ehrlich, Surf. Sci. Lett. **293**, L900 (1993).
[15] S. van Dijken, L. C. Jorritsma, and B. Poelsema, Phys. Rev. Lett. **82**, 4038 (1999).
[16] N. J. Shevchik, J. Non-Cryst. Solids **12**, 141 (1973).
[17] S. J. Linz, Eur. J. Phys. **16**, 67 (1995).
[18] M. Raible, S. G. Mayr, S. J. Linz, M. Moske, P. Hänggi, and K. Samwer, Europhys. Lett. **50**, 61 (2000).
[19] H. Kallabis, L. Brendel, J. Krug, and D. E. Wolf, Int. J. Mod. Phys. B **11**, 3621 (1997).
[20] K. Moser, J. Kertész, and D. E. Wolf, Physica A **178**, 215 (1991); J. G. Amar and F. Family, Phys. Rev. A **41**, 3399 (1990); C.-H. Lam and F. G. Shin, Phys. Rev. E **58**, 5592 (1998).